



Benchmarking of Different Inverse Point Kinetics Implementations for an Autocorrected Reactimeter Algorithm

April 2024

Changing the World's Energy Future

Paul Alexandre Ferney, Mark D DeHart



DISCLAIMER

This information was prepared as an account of work sponsored by an agency of the U.S. Government. Neither the U.S. Government nor any agency thereof, nor any of their employees, makes any warranty, expressed or implied, or assumes any legal liability or responsibility for the accuracy, completeness, or usefulness, of any information, apparatus, product, or process disclosed, or represents that its use would not infringe privately owned rights. References herein to any specific commercial product, process, or service by trade name, trade mark, manufacturer, or otherwise, does not necessarily constitute or imply its endorsement, recommendation, or favoring by the U.S. Government or any agency thereof. The views and opinions of authors expressed herein do not necessarily state or reflect those of the U.S. Government or any agency thereof.

Benchmarking of Different Inverse Point Kinetics Implementations for an Autocorrected Reactimeter Algorithm

Paul Alexandre Ferney, Mark D DeHart

April 2024

**Idaho National Laboratory
Idaho Falls, Idaho 83415**

<http://www.inl.gov>

**Prepared for the
U.S. Department of Energy
Under DOE Idaho Operations Office
Contract DE-AC07-05ID14517**

Benchmarking of Different Inverse Point Kinetics Implementations for an Autocorrected Reactimeter Algorithm

Paul A. Ferney,* Mark D. DeHart,†

*Fuel Development, Performance & Qualification, Idaho National Laboratory, 1955 N Fremont Ave, Idaho Falls, ID 83415, paul.ferney@inl.gov

†Reactor Physics Methods & Analysis, Idaho National Laboratory, 1955 N Fremont Ave, Idaho Falls, ID 83415, mark.dehart@inl.gov

INTRODUCTION

In November 2017, the Transient Reactor Test Facility returned to operation. Since that time, many transient test series have been completed, such as the Transient Heatsink Overpower Response capsule (THOR) [1], the Transient Water Irradiation System for TREAT (TWIST) [2], and Sirius [3]. Each has provided valuable data for materials performance and reactor safety that can be applied in future designs. During each experimental series, detector count rates provided important information on the core behavior during transients. However, a limitation of these data is that variations in the neutron distribution during experiments can cause errors when attempting to infer reactivity evolution from detector signals. Neutron physics codes can be used to compute the flux shape variations [4]. However, this is a poor solution when the experimental data is used for code verification, validation and uncertainty quantification. Indeed, if the output of the code is used both as a reference and to correct what the reference is compared to, the circular dependency limits the quality of the verification, validation and uncertainty quantification approach.

To overcome this problem, the autocorrected reactimeter algorithm (ACRA) has been developed [5]. This approach infers a time-dependent reactivity evolution by testing different spatial corrections and selecting the one that minimizes reactivity variations when the core is in a frozen configuration (i.e., when there is no variation in parameters affecting reactivity). However, the scope of this method was limited to transients where there were negligible thermal feedback. Indeed, the core is never in a frozen configuration when the fuel temperature varies during the whole transient. This is our motivation for developing an improved version of the ACRA that does not require frozen configurations.

To develop this new algorithm, we need a precise and unbiased implementation of the inverse point kinetic equations (IPKEs) as any error in the reactivity evaluation will be propagated into the choice of the optimal spatial correction. Indeed, the previous reactimeter algorithm would use approximations, such as a negligible flux amplitude derivative, to focus on rapidity [6]. For the numerical validation of ACRA, we aim at absolute error under $10^{-3} pcm$ for reactivity derived from signals similar to the one of this study.

In this summary, we test eight different IPKE implementations. Each will process a mockup signal built for this study, similar to those that the future ACRA will process. Each reactivity output will be compared to the reference reactivity that has been used to generate the mockup signal. The implementation minimizing the difference with the reference reactivity will be used in the development of a new ACRA formulation.

THEORY

Inverted Point Kinetics Equations

The eight-group point kinetic equations are:

$$\dot{N}(t) = \frac{\rho(t) - \beta}{\Lambda} N(t) + \sum_{i=1}^8 \lambda_i c_i(t) \quad (1)$$

and

$$\dot{c}_i(t) = \frac{\beta_i}{\Lambda} N(t) - \lambda_i c_i(t) \quad (2)$$

with:

- N , the flux amplitude,
- c_i , the quantity of precursors from the i^{th} family,
- $\rho(t)$, the time-dependent reactivity,
- λ_i , the decay constant associated with the i^{th} family of precursor,
- β_i , the delayed neutron fraction associated with the i^{th} family of precursor,
- $\beta = \sum \beta_i$, the total fraction of delayed neutron,
- Λ , the neutron mean generation time.

The kinetic parameters used in this study are displayed Table I.

TABLE I. Mean and standard deviation of reactivity difference sets

Parameter	Value	Parameter	Value
β	760 pcm	Λ	25 μs
β_1	23 pcm	λ_1	0.0125 s ⁻¹
β_2	131 pcm	λ_2	0.0283 s ⁻¹
β_3	78 pcm	λ_3	0.0425 s ⁻¹
β_4	124 pcm	λ_4	0.133 s ⁻¹
β_5	276 pcm	λ_5	0.292 s ⁻¹
β_6	14 pcm	λ_6	0.667 s ⁻¹
β_7	97 pcm	λ_7	1.63 s ⁻¹
β_8	17 pcm	λ_8	3.55 s ⁻¹

IPKEs are implemented such as:

$$\rho(t) = \Lambda \frac{\dot{N}(t) + \sum_{i=1}^8 \dot{c}_i(t)}{N(t)}, \quad (3)$$

and

$$\dot{c}_i(t) = \frac{\beta_i}{\Lambda} N(t) - \lambda_i c_i(t). \quad (4)$$

When discretizing these equations, three issues arise:

1. **The next step quantity of precursors calculation.** The first approach possible (**proportional difference**) is to assume that the quantity of precursor is linear between t_{k+1} and t_k . Thus, the derivative is constant, and the precursor variation is proportional to Δt . The second approach (**exponential difference**) is to assume that only the flux amplitude N is constant between t_{k+1} and t_k . Therefore, the precursor equations (Eq. (2)) becomes a first-order differential equation with exponential solutions.
2. **The flux amplitude definition in the precursor equation.** The flux amplitude is included in the precursor equation (4). We can use the flux amplitude value of the next computed step $N(t_{k+1})$ (**implicit precursors**) or use the value of the previous step $N(t_k)$ (**explicit precursors**).
3. **The flux amplitude definition at the denominator.** The expression of reactivity (Eq. (3)) includes the value of the flux amplitude in the denominator. We can use the flux amplitude value of the next computed step $N(t_{k+1})$ (**implicit denominator**) or use the value of the previous step $N(t_k)$ (**explicit denominator**).

On the one hand, the proportional difference approach led to the following precursors variation definition:

$$\Delta c_i = c_i(t_{k+1}) - c_i(t_k) = \Delta t \left(\frac{\beta_i}{\Lambda} N - \lambda_i c_i(t_k) \right), \quad (5)$$

where $\Delta t = t_{k+1} - t_k$.

On the other end, the exponential difference approach led to the following precursors variation definition:

$$\Delta c_i = c_i(t_{k+1}) - c_i(t_k) = \left(1 - e^{-\lambda_i \Delta t} \right) \left(\frac{\beta_i}{\lambda_i \Lambda} N - c_i(t_{k-1}) \right). \quad (6)$$

Finally, eight different combinations can be implemented :

1. Explicit precursors, explicit denominator, proportional difference.
2. Implicit precursors, explicit denominator, proportional difference.
3. Explicit precursors, implicit denominator, proportional difference.
4. Implicit precursors, implicit denominator, proportional difference.
5. Explicit precursors, explicit denominator, exponential difference.
6. Implicit precursors, explicit denominator, exponential difference.
7. Explicit precursors, implicit denominator, exponential difference.
8. Implicit precursors, implicit denominator, exponential difference. This implementation is also used in recent work [7].

An example of reactimeter algorithm workflow is displayed Fig. 1.

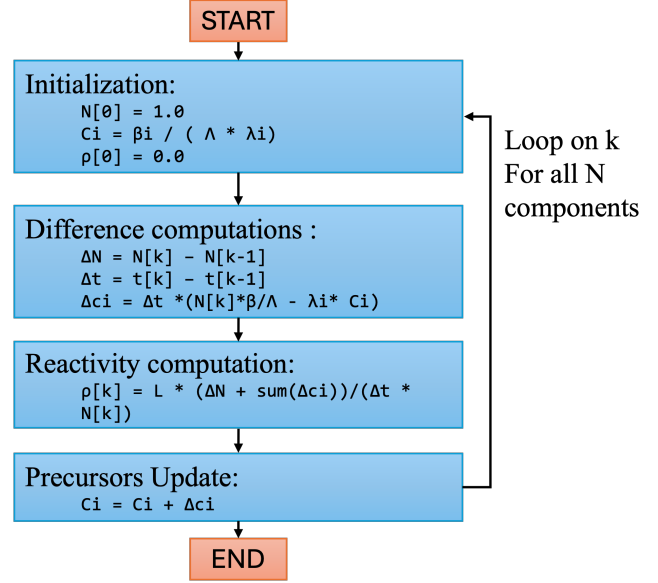


Fig. 1. Reactimeter algorithm workflow - Implicit precursors, implicit denominator, proportional difference

Mockup signal

To test the different implementation of the reactimeter algorithm, we do not use a measured experimental signal. We manufacture a mockup signal based on a well-defined reactivity curve. The mockup signal corresponds to a linear increase of positive reactivity insertion at a rate of $0.1 pcm/s$ combined with four negative reactivity insertion steps of $50 pcm$ each. The *Radau* method of the *SciPy* Python library was used to solve the point kinetic equations and generate the signal. A constant time step of $0.1s$ is used. The reference reactivity used to generate the signal is displayed Fig. 2, and the generated signal is displayed in Fig. 3.

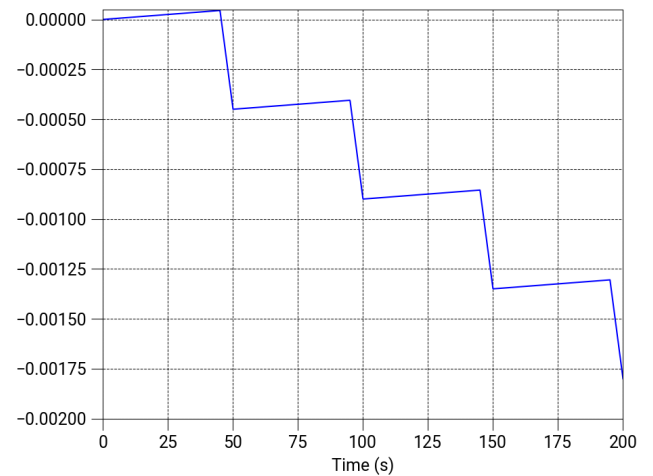


Fig. 2. Reference reactivity used to generate the signal

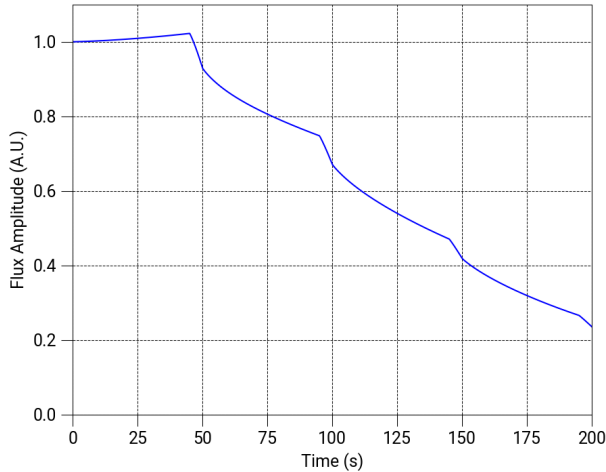


Fig. 3. Generated signal

Results and Analysis

The difference between each reactivity and the reference reactivity is displayed in Fig. 4 and Fig. 5. The mean and standard deviation of each reactivity difference set is displayed in Table II. The lower the mean, the more unbiased the implementation. The lower the standard deviation, the more precise the implementation. For example, Implementation 3 appears to be unbiased but not precise.

TABLE II. Mean and standard deviation of reactivity difference sets

Implementation	Mean (pcm)	Standard Deviation (pcm)
1	$+7.81 \times 10^{-2}$	2.68×10^{-1}
2	$+5.96 \times 10^{-2}$	7.85×10^{-2}
3	$+6.79 \times 10^{-3}$	2.31×10^{-1}
4	-1.19×10^{-2}	4.45×10^{-2}
5	$+9.00 \times 10^{-2}$	2.99×10^{-1}
6	$+7.14 \times 10^{-2}$	8.13×10^{-2}
7	$+1.86 \times 10^{-2}$	2.62×10^{-1}
8	-1.32×10^{-5}	7.54×10^{-4}

The implementation that output the reactivity closest to the reference is by far the one that uses both implicit definition for flux amplitude and exponential difference. This implementation is 300× more precise and 50× times less biased than any other implementation. Using an implicit definition of flux amplitude has the largest impact on reactivity precision (see Table II). Using both the exponential difference and the implicit denominator definitions improve the reactivity estimation when reactivity variation are important (see Fig. 5).

CONCLUSIONS

Different implementations of IPKE have been tested in this study. The implementation using only implicit definition of the flux amplitude and exponential difference for precursors outperform every other implementation tested in this study.

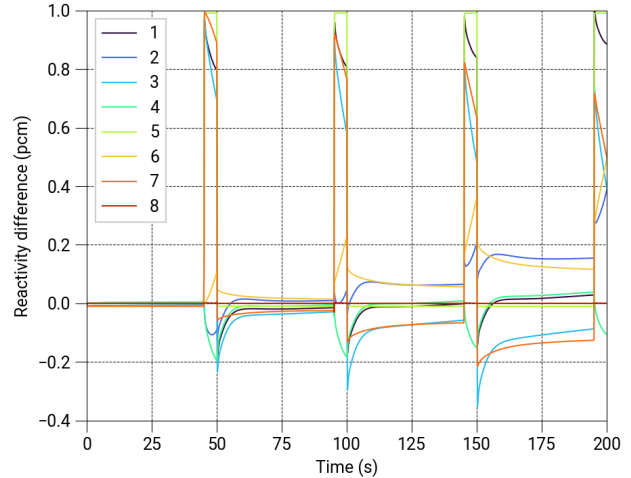


Fig. 4. Difference between computed reactivity and reference reactivity for each implementation

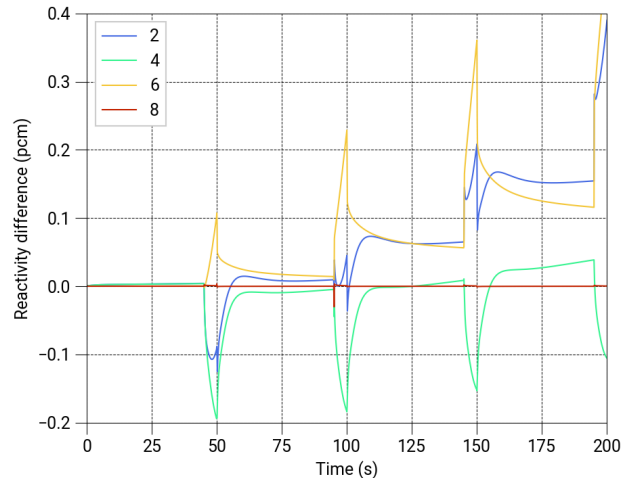


Fig. 5. Difference between computed reactivity and reference reactivity for implicit precursors implementation

The bias of this implementation is 10^{-5} pcm regarding the signal generated in this study. The reactivity calculated at each time step is 10^{-3} pcm, accurate to within one sigma. This meets the requirements to build a new version of the ACRA to process signals similar to the one of this study. Furthermore, several characteristics of real detector signals such as noise, spatial and spectral variation of the flux have a significantly greater impact on the overall precision of the reactimeter algorithm than numeric errors related to implementation.

The real-world effects on the detector signals will be investigated while performing numerical validation of the new ACRA version, which is our immediate future work.

REFERENCES

1. N. WOOLSTENHULME, G. L. BEAUSOLEIL, C. JENSEN, C. PETRIE, and D. WACHS, "Irradiation

- Testing Methods for Fast Spectrum Reactor Fuels and Materials in DOE's Thermal Spectrum Test Reactors," in A. N. SOCIETY, editor, "2021 ANS Virtual Annual Meeting," (2021).
2. C. P. FOLSOM, R. J. ARMSTRONG, N. E. WOOLSTENHULME, D. D. IMHOLTE, K. S. ANDERSON, and C. B. JENSEN, "Thermal-hydraulic and Fuel Performance Scoping Studies of a Flowing Water Capsule in TREAT," in "TopFuel 2022," (10 2022).
 3. T. JING, S. SCHUNERT, V. M. LABOURÉ, M. D. DEHART, C.-S. LIN, and J. ORTENSI, "Multiphysics Simulation of the NASA SIRIUS-CAL Fuel Experiment in the Transient Test Reactor Using Griffin," *Energies*, **15**, 17 (2022).
 4. P. FERNEY, G. TRUCHET, R. BOFFY, J. TOMMASI, and J.-M. PALAU, "Comparing dynamic and quasi-static methods for rod-drop transients with TRIPOLI-4@," *Annals of Nuclear Energy*, **170**, 108993 (2022).
 5. P. FERNEY, G. TRUCHET, R. BOFFY, B. GESLOT, and J.-M. PALAU, "A spatially auto-corrected reactimeter algorithm," *Progress in Nuclear Energy*, **165**, 104912 (2023).
 6. Y. SHIMAZU, Y. NAKANO, Y. TAHARA, and T. OKAYAMA, "Development of a Compact Digital Reactivity Meter and a Reactor Physics Data Processor," *Nuclear Technology*, **77** (jun 1987), (Accessed on 12/06/2023).
 7. Y. SHIMAZU and W. VAN ROOIJEN, "Qualitative performance comparison of reactivity estimation between the extended Kalman filter technique and the inverse point kinetic method," *Annals of Nuclear Energy*, **66**, 161–166 (2014).